Frascati Physics Series Vol. XXIV (2002), pp. 261-277
INTERNATIONAL SCHOOL OF SPACE SCIENCE - 2001 Course on
ASTROPARTICLE AND GAMMA-RAY PHYSICS IN SPACE, L'Aquila (Italy), 30/8 - 7/9, 2001

THE ALPHA MAGNETIC SPECTROMETER, A PARTICLE PHYSICS EXPERIMENT IN SPACE

Roberto Battiston
Dipartimento di Fisica dell' Universitá and Sezione INFN
Via Pascoli, 06100 Perugia, Italy

ABSTRACT

The Alpha Magnetic Spectrometer (AMS) is a state of the art detector for the extraterrestrial study of matter, antimatter and missing matter. During the STS-91 precursor flight in may 1998 AMS collected nearly 100 millions of Cosmic Rays on Low Earth Orbit, measuring with high accuracy their composition. We present results on the flux of proton, electron, positron and helium. Analyisis of the under cutoff spectra indicates the existence of a new type of belts of energetic trapped particles characterized by a dominance of positrons versus electrons.

1 Introduction

The disappearence of the antimatter [1, 2, 3] and the presence at all scales in our universe of a non luminous components of matter (dark matter) [4, 5]

are two of the most intriguing misteries in our current understanding of the structure of the Universe.

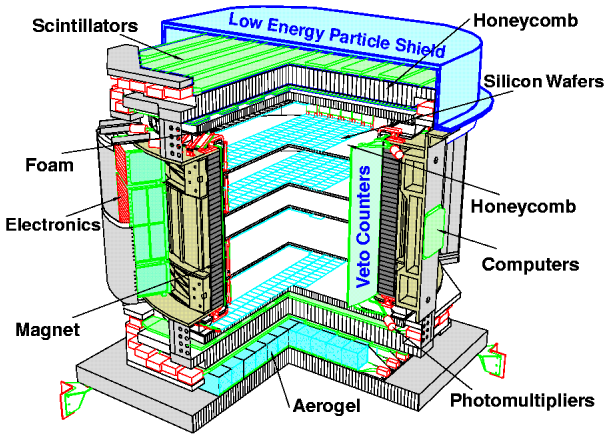

Figure 1: *AMS on the Discovery STS 91 precursor flight, June 1998.*

To study these problems, a high energy physics experiment, the Alpha Magnetic Spectrometer (AMS) [6], is scheduled for installation on the International Space Station in 2004. Goal of AMS is to perform a three year long measurement, with the highest accuracy, of the composition of Cosmic Rays in the rigidity range 0,1 GV to several TV. In preparation for this long duration mission AMS flew a ten days precursor mission on board of the space shuttle Discovery mission STS-91 in June 1998. This high statistics measurement of CR in space, enabled, for the first time, the systematic study the behaviour of primary CR near Earth in the rigidity interval from $0,1\ GV$ to $200\ GV$, at all longitudes and latitudes up to $\pm 51.7^o$. In this paper we present some relevant results obtained by AMS during the precursor mission. We also report the observation of high energy radiation belts in the near Earth region and on their composition, which shows remarkable differences with previously observed belts of trapped particles around our planet.

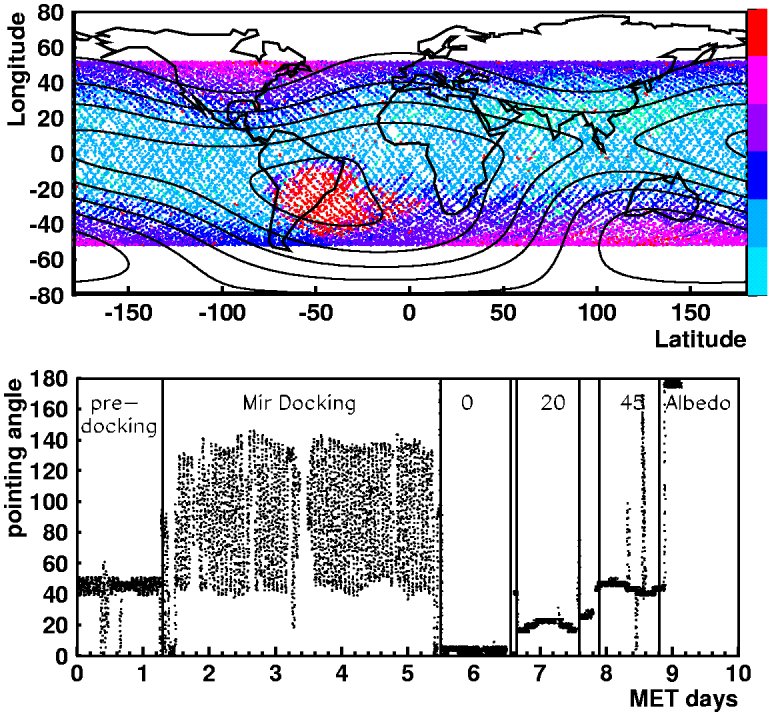

Figure 2: *(a)C.R. rates versus shuttle orbits (b) and shuttle attitudes during the STS91 mission as a function of the Mission Elapsed Time (MET).*

2 The AMS experiment on the STS-91 mission

Search of antimatter requires the capability to identify with the highest degree of confidence, the mass of particle traversing the experiment together with the absolute value and the sign of its electric charge.

The AMS configuration flown in 1998 on the Shuttle Discovery (Fig.1) includes a permanent Magnet, Anticounter (ACC) and Time of Flight (ToF) scintillator systems, a large area, high accuracy Silicon Tracker and an Areogel Threshold Cherenkov counter. The magnet is based on recent advancements in permanent magnetic material and technology which make it possible to use very high grade Nd-Fe-B to build a permanent magnet with $BL^2 = 0.15\ Tm^2$ weighting $\leq$ 2 tons. A charged particle traversing the spectrometer triggers the experiment through the ToF system, which measures the particle velocity with a resolution of $\sim 120\ ps$ over a distance of $\sim\ 1.4\ m$ [11].

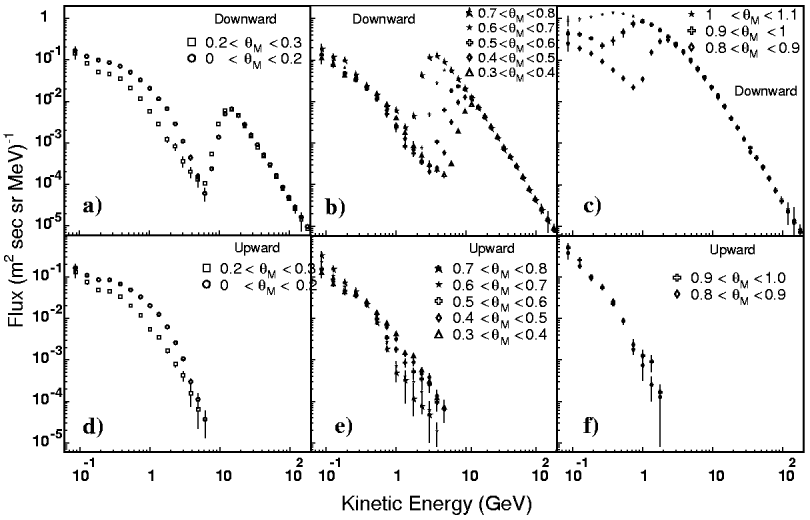

Figure 3: *Proton spectra measured by AMS for different geomagnetic latitude intervals.*

The pattern recognition and tracking is performed using the large area ($\sim$ 7 m^2), high accuracy Silicon Tracker [7, 9], which, for the Space Station mission, will be covered with 2300, high purity, double sided, 300 μm thick silicon wafers [12], following the technology developed in Italy by INFN for the Aleph [10] and L3 [8] vertex detectors at LEP. The active area of the AMS Silicon Tracker is about an order of magnitude larger than in the case of the microstrip silicon detectors presently installed at high energy Colliders. AMS is the first high energy spectrometer based only a high precision multilayer Silicon Tracker.

The momentum resolution for AMS on on the precursor mission was about ($\frac{\Delta p}{p} \sim 7\%$) at 10 GV, reaching ($\frac{\Delta p}{p} \sim 100\%$) at about 500 GV.

Four ToF scintillators layers and up to eight Silicon Tracker layers measure $\frac{dE}{dx}$, allowing a multiple determination of the absolute value of the particle charge.

By combining the various measurement it is then possible to determine the type of particle traversing the magnet and identify interesting particles with a background rejection which for anti-matter searches is expected to reach one part in 10 billions.

During the period june 2^{nd} to june 12^{th}, 1998 the Shuttle Discovery has performed 154 orbits at an inclination 51.7^o and at an altitude varying between 390 to 350 km. During the mission AMS collected a total of about 100 Million triggers, at various Shuttle attitudes (Fig.2). In the Figure one notice the period of Shuttle to Mir docking when the Shuttle attitudes are rapidly changing with time.

Almost all results published so far [13, 14, 15] were obtained with data collected during well defined attitude periods with AMS pointing at $0^o, 20^o$ and 45^o with respect to zenith (deep space).

These data are the first high quality CR data collected with a magnetic spectrometer located outside the atmosphere. The measurements cover all geomagnetic longitudes and most latitudes. These data allow a direct and accurate measurement of the CR composition and spectra, as well as a systematic study of the effects of the geomagnetic field.

The measurement of the proton flux as a function of the geomagnetic latitude (Fig. 3a-3c), shows that, in addition to the primary CR spectrum visible above the geomagnetic cutoff, there is a substantial second spectrum, extending to much lower energy and exhibiting some significant latitude dependence close to the equator. These particles cannot come from the deep space, they are on forbidden orbits, but are produced in the interaction of the primary CR with the top layers of the atmosphere. A characteristic of the second spectrum is that it is up-down symmetric (Fig. 3d-3f).

Second spectra with similar geomagnetic latitude dependence have been detected by AMS in the low energy region of the spectra of e^-, e^+ [16], D [17] and, although with weaker intensity, ^3He. Fig. 4 and 5 show the results for electrons, positrons and Helium. These results on the second spectra are discussed later in the paper.

Adding all data collected above the geomagnetic cutoff it is possible to obtain a precise estimate of the primary CR differential flux. Parametrizing the omnidirectional CR flux as $\Phi(R) = \Phi_o R^\gamma$ (R in GV) we obtain the results reported in Table 1.

It it interesting to compare the AMS measurement of the primary fluxes with previous results obtained with stratospheric balloons [18, 19, 20, 21, 22]. Fig.7 shows the comparison for the proton spectrum, multiplied by $E^{2.5}$. The improved statistical significance and the wider energy interval covered by AMS

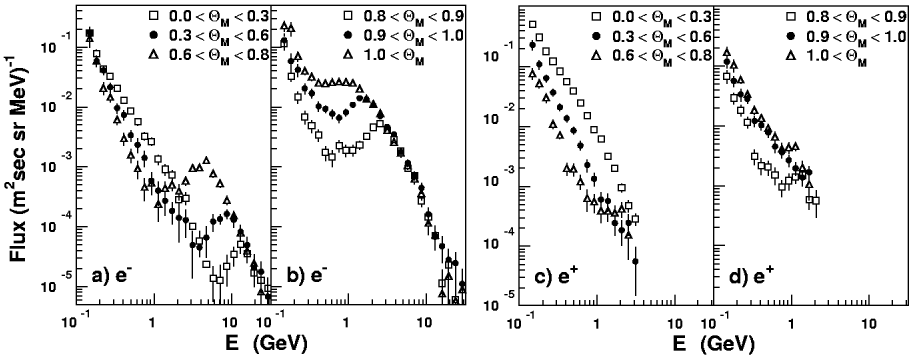

Figure 4: *Electrons and positron spectra measured by AMS during the STS91 flight.*

Table 1: *AMS results on the parametrization of proton and helium primary flux.*

Proton flux	
γ	2.78 ± 0.009 (fit) ± 0.019 (syst)
Φ_o	17.1 ± 0.15(fit) ± 1.3(syst) $\pm 1.5(\gamma) GV^{2.78} (m^2 s\ srMeV)^{-1}$
Helium flux	
γ	2.740 ± 0.010(fit)± 0.016(syst)
Φ_o	2.52 ± 0.09(fit)± 0.13 (syst) $\pm 0.14(\gamma) GV^{2.78} (m^2 s\ srMeV)^{-1}$

data is evident: thanks to the improved accuracy obtained with only few days in space, it is possible to clarify the situation resulting from the data published over the last 15 years by the various Collaborations using different implementations of the NASA New-Mexico spectrometer [19, 20, 21, 22] and by the Bess Collaboration [18].

Similar consideration apply for the comparison of the measurement of Helium primary flux (Fig.7).

Both for protons as well as for Helium, AMS show a nice agreement with the measurement of the Bess Collaboration [18], although our data have a smaller statistical error and extends over a wider energy interval. Using the

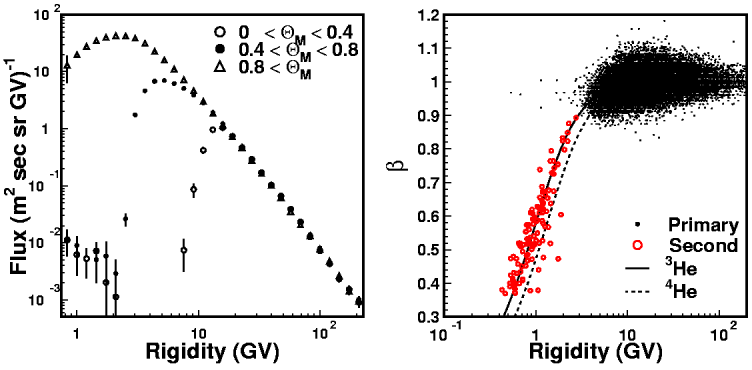

Figure 5: *Helium spectra measured by AMS during the STS91 flight.*

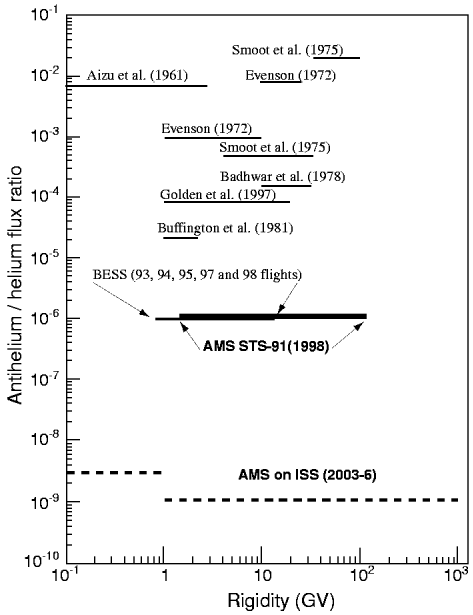

Figure 6: *Antimatter limits.*

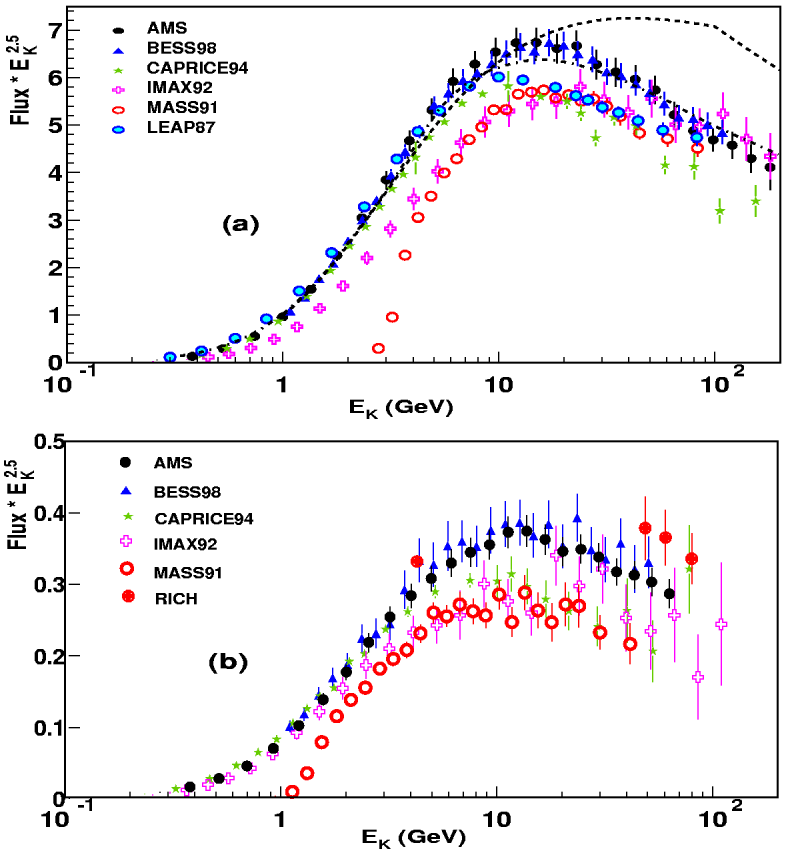

Figure 7: *(a)Primary proton flux measured by AMS and compared with existing balloons measurements. The lines are parametrizations of the primary cosmic rays used in atmospheric ν flux calculation: dashed line HPPK [23], dot-dashed line Bartol group [24]; (b) primary He flux measured by AMS and compared with existing balloons measurements.*

Figure 8: *Motion of charged particles in the geomagnetic belts. A) gyration B) bouncing C) drift.*

large He sample collected by AMS a search for anti-He candidates has also been performed. Within 2.3 Millions He events no anti-He candidates have been found, up to a rigidity of 140 GV.

Assuming identical He and anti-He spectra we obtain a model independent upper limit of $1.1 10^{-6}$ over the rigidity interval 1 to 140 GV, which can be compared to previous results (Fig.7).

3 Observation of high energy particle belts

The trapping of charged particles in the quasi dipolar earth magnetic field is a classical problem, which has been studied in great detail [27] following Van Allen observations in 1958 [29]. The basic physical mechanism is well understood. For sufficiently low rigidities, the trapped particles spiralize along orbits defining shells surrounding our planet.

These shells are shaped along the magnetic field lines and are roughly symmetric in latitude with respect to the geomagnetic equator (Fig.8). The motion of a trapped particle can be separated in three components, the revolution around the guiding center or gyration, the bouncing between mirror points located $\approx$ symmetrically with respect to the geomagnetic equator (magnetic bottle), and a longitudinal drift around the earth. The geometrical locations

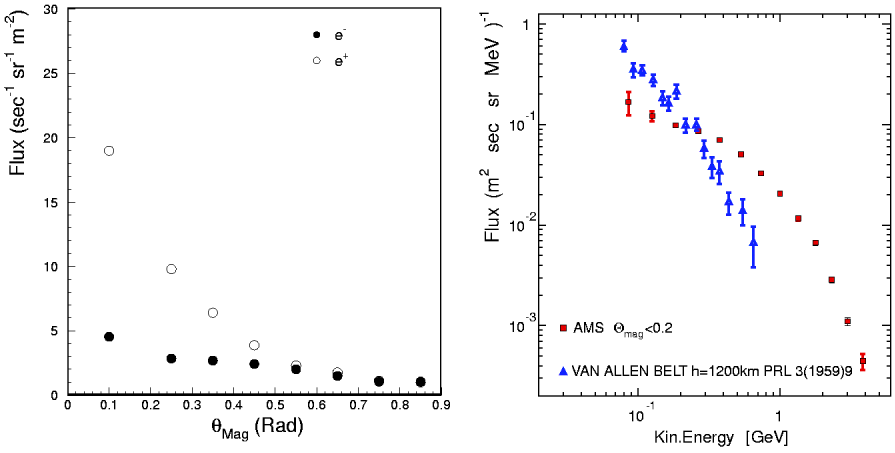

Figure 9: *(a)$\frac{e^+}{e^-}$ ratio inside the belts observed by AMS, as a function of the geomagnetic latitude; (b)comparison among a typical Van Allen belt proton spectrum and equatorial AMS belts proton spectrum.*

defined by the orbits of trapped particles are called shells.A shell can be univocally determined by two parameters. For example a pair of variables are L, the distance of the shell at the equator measured in unit of the Earth radius ($R_\oplus$), and B_{mir}, the value of the magnetic field at the point where the particles reverse their motion (mirror point) [30]. Depending on the shell, B_{mir} can be locally very deep the atmosphere (it can be below the earth crust). Shells which are characterized by these value of B_{mir} cannot trap the particles, since they are lost within one or few bounces across the magnetic equator.

A particle belonging to a shell will remain on the same shell until it is disturbed by (a) interaction with the top layers of the atmosphere or other particles or (b) interaction with electrical or magnetic variable field.

Conversely, primary cosmic rays coming from deep space cannot enter a shell unless their trajectories are disturbed by some interaction with matter or fields. The existence of the shells is the result of the equilibrium between two mechanisms: some contributing to fill the shells with new particles and others removing some of the trapped particles.

Table 2: *Different types of particle belts around the Earth.*

Belt type	Particle type	Rigidity [MeV/n]	Filling mechanisms	L	Residence time [d]
Van Allen (inner)	p e^-	$0.1-100$ $0.01-1$	$n \to pe^-\overline{\nu}_e$, external belts	< 2.5	$10-1000$
Van Allen (outer)	e^- p	$1-10$ $0.1-1$	solar wind	> 2.5	$1-10$
SAMPEX	N^{+x}, O^{+x}, Ne^{+x}	10 $10-100$	Anomalous CR	2	$10-100$
AMS	p e^- e^+ ^3He	$100-1000$ $100-1000$ $100-1000$ $100-1000$	primary CR interacting with the *atmosphere*	≤ 1.15	$10^{-6}-10^{-4}$

If the dynamics of the particles trapped is well understood, the mechanisms contributing to shell stability are much less understood. They involve: interaction of high energy CR with the atmosphere creating neutrons which decays in flight, $n \longrightarrow p + e^- + \overline{\nu}_e + 782KeV$, filling the belts (CRAND mechanism [28]), instabilites due to solar storms, as well as other types of magnetic and electric instabilities. It should be pointed out, however, that the mechanisms proposed are compatible with the observed dominance of protons and electrons in the Van Allen belts.

The shell can be classified by their composition and location. The original Van Allen belts contain only proton and electrons and extend to very large distance from the earth, up to $L \approx 6$. Van Allen belts are divided into inner and outer belts, since there is a dip in the particle flux intensitiy at about 2.5 L. During the last 20 years, there have been reports of the observation of a low flux of trapped ions, mainly He and O, with traces of C e N, and having energies of a few MeV/n and $L = 3-4$. These particles are extracted from the upper layers of the atmosphere during solar storms. More recently, nearly 40 years after Van Allen discovery, the analysis of SAMPEX data [32] has shown the existence of belts included in the inner Van Allen belts, containing heavier nuclei like N, O, Ne with rigidities of the order of $10/MeV$.

The SAMPEX belts are different from the Van Allen belts mainly because of their composition due to a different the filling mechanism, which is likely

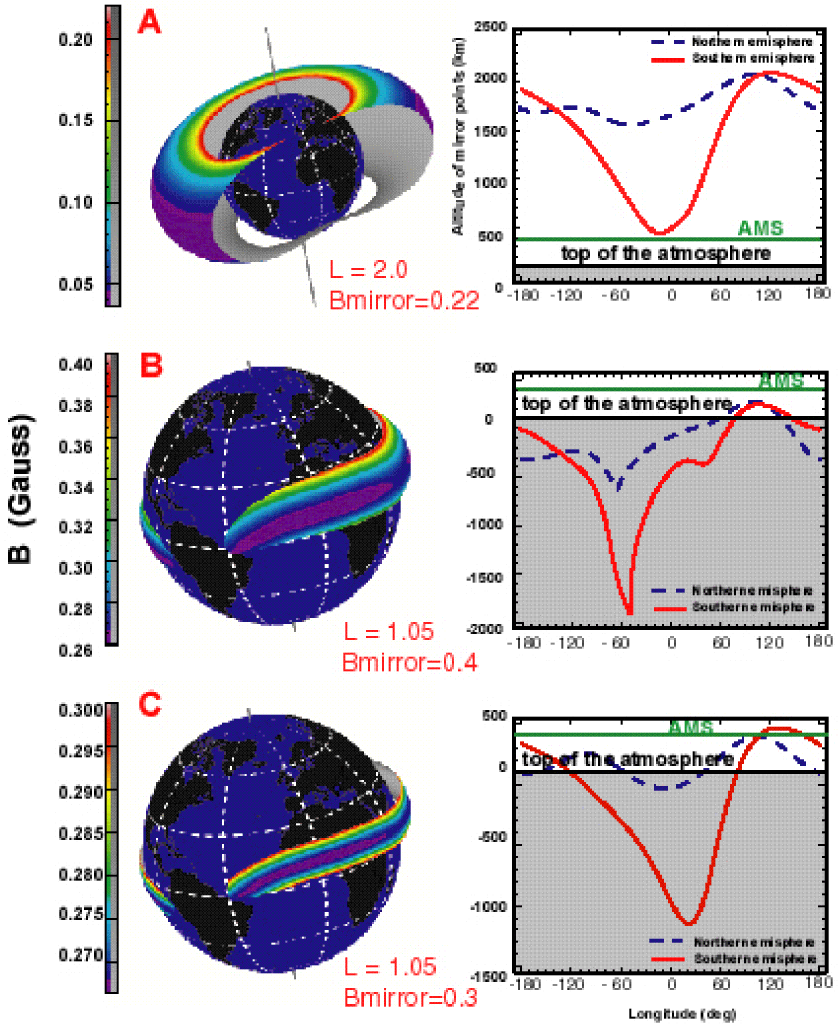

Figure 10: *Van Allen versus AMS belts. (A) Van Allen belts have high L values, B_{mirr} is located mainly above AMS orbits, particles weakly interact with the atmosphere and have lifetimes ranging from days to months. AMS belts have $L \leq 1.5$, and depending on the value of the B_{mirr} their lifetime ranges from fractions of a second (B) to several seconds (C).*

due to the interaction of the so called Anomalous Cosmic Rays with the Earth atmosphere [33, 31].

The belts observed by AMS are different in composition since they also contain a large fraction of positrons, but also deuterium and ^3He. These particles have not been observed in the Van Allen or SAMPEX belts. Particularly striking is the abundance of positrons versus electrons (Fig.4), with a ratio exceeding a factor of four in the equatorial region (Fig. 9a).

AMS observed shells with $L \leq 1.15$, well below the inner Van Allen belts. In the belts studied by AMS the observed proton spectrum is harder (Fig. 9b) than in the case of Van Allen belts. This can be understood since their location is closer to the earth and the particles do experience a stronger trapping field. Another difference with the Van Allen belts is the residence time of the trapped particles, computed using computer based tracing techniques, which is in the region of seconds and not days or weeks. These shells cannot be observed by stratospheric balloons, since their mirror fields are above the atmosphere except in correspondence of the South Atlantic Anomaly. It follows that the observed particles do not belong to the various types of albedo particles reported in the past by experiments on balloons.

In Table 2 we summarize the main features of the different type of belts identified during the last 40 years. As we can see the situation is very varied, corresponding to different filling mechanisms. Since we are dealing with continuous distributions, the reported intervals (rigidity, L, residence time) should be taken as typical order of magnitudes. In Fig.10, we compare the structure of the AMS belts to the Van Allen belts as well as the dependence of the mirror field altitude with the longitude.

4 Conclusions

The first mission of the Alpha Magnetic Spectrometer, although lasting only ten days, has been scientifically very rewarding, allowing for the first time a very detailed measurement of high energy cosmic rays outside the atmosphere. In addition to the most accurate measurements obtained so far for the primary flux of $p, e^+, e^-, D, ^3He$ and ^4He spectra over most of the earth surface, these results have shown the existence of a substantial second spectrum of high energy particles trapped within low altitude belts. These new belts have a very characteristic composition, dominated by positively charged particles, mainly

Table 3: *Physics capabilities of AMS after three years on the ISS*

Elements	Sensitivity	(Now)	Energy Range(GV)	Physics
e^+	10^8	$(\sim 10^3)$	$0.1-100$	$\uparrow$
$\bar{p}$	500000	(~ 30)	$0.5-100$	Dark Matter
γ			$0.1-300$	$\downarrow$
He/He	$\frac{1}{10^9}$	$(\frac{1}{10^5})$	$0.5-20$	Antimatter
$\bar{C}/C$	$\frac{1}{10^8}$	$(\frac{1}{10^4})$	$0.5-20$	CP, GUT, EW
D, H_2	10^9		$1.0-3.0$	$\uparrow$
$^3He/\ ^4He$	10^9		$1.0-3.0$	Astrophysics
$^{10}Be/\ ^9Be$	2%		$1.0-3.0$	$\downarrow$

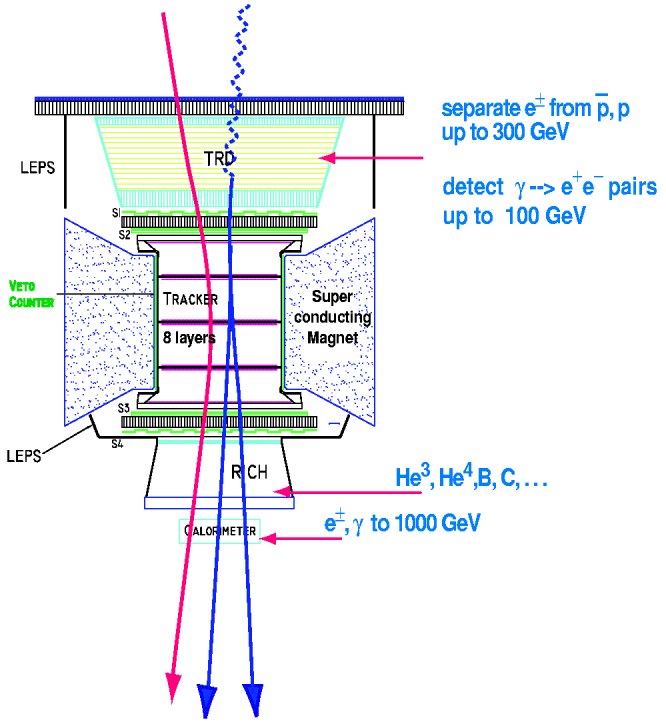

Figure 11: *Configuration of AMS on the ISS for the three years mission scheduled on UF4 in 2004.*

p, e^+ and D. Their existence should be taken into account when calculating radiation doses for astronauts on the ISS or background rates for low orbit satellites.

AMS is currently being refurbished to be ready for a three years mission with UF4 in 2004.A stronger magnetic field from a superconducting magnet, $B = 0,7\ T$, a fully equipped Silicon Tracker, together with three powerful particle identification detectors, a Transition Radiation Detector, a Ring Imaging Cherenkov (RICH) detector and an Electromagnetic Calorimeter, will allow precise particle identification up to $O(TeV)$ of energy (Fig.11). The physics capabilities of AMS after three years of exposure on the ISS are summarized in Table 3. AMS will be the only large acceptance magnetic facility which will be exposed for long time in space. It will allow a measurements of the flux and composition of Cosmic Rays with an accuracy orders of magnitude better than before. The large improvement in sensitivity given by this new instrument, will allow us to enter into a totally new domain to explore the unknown.

5 Acknowledgment

This work has been partially supported by the Italian Space Agency (ASI) under contract ARS-98/47.

References

1. Steigmann, G., Ann. Rev. Astron. Astroph., **14** p. 339, 1976.

2. Kolb, E.W., Turner, M.S., Ann. Rev. Nucl. Part. Sci. **33** p. 645, 1983.

3. Peebles, P.J.E., Principles of Physical Cosmology, Princeton University Press, Princeton N.J., 1993.

4. Ellis, J. et al., Phys. Lett. **B214**, p. 403, 1988.

5. Turner, M.S., Wilzek, F., Phys. Rev. **D42**, p. 1001, 1990.

6. Ahlen, S. et al., Nucl. Inst. Meth. **A350**, p. 351, 1994.

7. Battiston, R., Nucl. Instr. Meth. (Proc. Suppl.) **B44**, p. 274, 1995.

8. Acciarri, M. et al., Nucl. Inst. Meth. **A289** p. 351-355, 1990.

9. Alcaraz, J. et al., Il Nuovo Cimento **112A**, p. 1325-1344, 1999.

10. Batignani, G. et al., Nucl. Inst. Meth. **A277** p. 147, 1989.

11. Alvisi, D. et al., Nucl. Inst. Meth. **A437** p. 212, 1999.

12. Produced at CSEM, SA Rue J. Duot 1, P.O. Box, CH-2007 Neuchatel, http://www.csem.ch.

13. AMS Collaboration, Alcaraz, J. et. al., Search for Antihelium in Cosmic Rays, Phys. Lett. **B461**, p. 287, 2000.

14. AMS Collaboration, Alcaraz, J. et. al., Protons in Near Earth Orbit, Phys. Lett. **B472**, p. 215, 2000.

15. AMS Collaboration, Alcaraz, J. et. al., Leptons in Near Earth Orbit, Phys. Lett. **B484**, p. 10, 2000.

16. AMS Collaboration, Alcaraz, J. et. al., Cosmic Protons, Phys. Lett. **B490**, p. 27, 2000.

17. Lamanna, G. PhD Thesis, University of Perugia, October 2000, unpublished.

18. BESS98, Sanuki, T. et al., astro-ph/0002481, 2000.

19. CAPRICE94, Boezio, M. et al., ApJ **518**, p. 457, 1999.

20. IMAX92, Menn, W. et al., The Astroph. J. **533**, p. 281, 2000.

21. MASS91, Bellotti, R. et al., Phys. Rev. **D60**, p. 052002, 1999.

22. LEAP87, Seo, E.S. et al., ApJ **378**, p. 763, 1991.

23. HPPK, Honda, M. et al., Phys. Rev. **52**, p. 4985, 1995.

24. BARTOL, Lipari, P. and Stanev, T., Talk given at Now 2000 Conference, 2000.

25. Smoot, G.F. et al., Phys. Rev. Lett. **35** p. 258-261, 1975; Steigman, G. et al., Ann. Rev. Astr. Ap. **14** p.399, 1976; Badhwar, G. et al., Nature **274** p. 137, 1978; Buffington, A. et al., ApJ **248** p. 1179-1193, 1981; Golden, R.L. et al., ApJ **479** p. 992, 1997; Ormes, J.F. et al., ApJL **482** p. 187, 1997; Saeki,T. et al., Phys. Lett. **B422** p. 319, 1998.

26. Nozaki, M., OG.1.1.23, 26th ICRC, Salt Lake City, Utah, 1999.

27. For a recent review see Walt,M., Radiation Belts Models and Standards, AGU Geophysical Monograph 97, p.1, 1997.

28. Singer,S.F., Phys. Rev. Lett. **1** p. 181, 1958; Hess, W.N., Phys. Rev. Lett.**3** p.11, 1959; Kellogg, P., J.Geophys. Res. **65** p. 2,705, 1960; Vernov, S.N. et al., Soviet Physics, Doklady **4** p.154, 1959.

29. Van Allen, Ludwig, Ray, and McIlwain, IGY Satellite Series Number 3, **73** Natl. Acad. Sci., Washington D.C., 1958; Van Allen, McIlwain, and Ludwig, J. Geophys. Research **64**, p. 271, 1959; Van Allen, J.A. and Frank. L.A., Nature **183** p. 430, 1959.

30. McIlwain, C.E., J.Geophys. Res. **66**p. 3681-3691, 1961.

31. Mewaldt, R.A., Radiation Belts Models and Standards, AGU Geophysical Monograph 97, p.35, 1997.

32. Cook, W.R., IEEE Trans. Geosci. Remote Sensing **31** p. 557-564, 1993.

33. Cummings, J.R. et al., Geophys. Res. Lett. **20** p. 2003-2006, 1993; Cummings, J.R. et al., IEEE Trans. Nucl. Sci. **40** p. 1459-1462, 1993.